32nd International Conference
ENGINEERING MECHANICS 2026
Medlov, Czech Republic, May 11 – 13, 2026

FLUCTUATION ANIZOTROPY OF ISOTHERMAL FLOW TROUGH NUCLEAR FUEL ROD BUNDLE MODEL WITH SWIRLER-MIXING GRIDS

Janský V.[1] **Duda D.**[2], **Uruba V.**[3] **Yanovych V.**[4],

Abstract: *This document describes the exploration of isothermal flow in nuclear fuel assembly performed at the University of West Bohemia in Pilsen. The spacer and mixing grids of the model fuel assembly are similar to the basic grids used at the VVER (vodo-vodjanoj energetičeskij reaktor), i.e. there are alternating nodes of circle shape and of tri-star shape. The tri-star is modified to create a swirling element, which produce longitudinal vortices in each even inter-rod channel. The fluctuation anisotropy coefficient F displays anisotropic turbulence almost everywhere. This analysis shows a significant contribution of the boundary layers formed at the fuel rods, because the turbulence in the vortex envelopes cannot evolve into full homogeneous and isotropic turbulence.*

Keywords: Particle Image Velocimetry, Nuclear Fuel Assembly, Fluctuation Anisotropy, Vortex

1. Introduction

The bundles of nuclear fuel rods in power reactors are tightly packed and supported by swirling mixing grids to maintain the required design geometry and enhance the mixing of the coolant. These grids are made from thin-walled structures with complex shapes. The geometry of the mixing vanes is important for coolant mixing, in order to normalize the flow velocity of the coolant while improve flow turbulence to break the boundary layer and enhance the heat removal produced in the fuel. In this study, we present an experimental investigation of isothermal air flow through a model rod bundle equipped with swirler-mixing grid of hexagonal symmetry that correspond with the VVER NPPs fuel. Using stereoscopic PIV (Tropea et al., 2007), we observed fluctuation anizotropy of the isothermal flow characterized through the downstream velocity fields.

2. Experimental setup

The measurement is performed inside the larger wind tunnel at the University of West Bohemia; the tunnel is not *large* in world-wide sense, but with test section of size $3.0 \times 0.3 \times 0.2\,\mathrm{m}^3$ is the largest one at the University of West Bohemia, see Yanovych et al. (2019). The velocity within the test section is $U = 20\,\mathrm{m/s}$. The mesh parameter, i.e. the distance between neighboring fuel rods, is $M = 59.1\,\mathrm{mm}$, thus the Reynolds number based on M is $\mathrm{Re}_M = 7.34 \cdot 10^4$. However, in many studies focusing to nuclear fuel assembly experiments such as Nguyen et al. (2019); Turankok et al. (2024); Nazififard (2018), the Reynolds number is defined by using *hydraulic diameter*, which is for hexagonal symmetry equal to

$$D_h = 4 \cdot \frac{\text{Area of free cross-section}}{\text{Length of boundary of free cross-section}} = D \cdot \left(\frac{2\sqrt{3}}{\pi} \left(\frac{M}{D} \right)^2 - 1 \right) = 49.1\,\mathrm{mm} \qquad (1)$$

[1] Ing. Vojtěch Janský: Elektrárna Dukovany II, a. s.; Duhová 2; 140 00, Prague; CZ, vjansky@fst.zcu.cz
[2] Ass. Prof. RNDr. Daniel Duda, Ph.D.: Faculty of Mechanical Engineering, University of West Bohemia in Pilsen, Univerzitní 22; 306 14, Pilsen; CZ, dudad@fst.zcu.cz
[3] Prof. Ing. Václav Uruba, CSc.: Faculty of Mechanical Engineering, University of West Bohemia in Pilsen, Univerzitní 22; 306 14, Pilsen; CZ, uruba@fst.zcu.cz
[4] Ass. Prof. Ing. Vitalii Yanovych, DrSc.: Faculty of Mechanical Engineering, University of West Bohemia in Pilsen; Univerzitní 22; 306 14, Pilsen; CZ, yanovych@fst.zcu.cz

ISSN: 1805-8256, doi: 10.21495/em2026-57

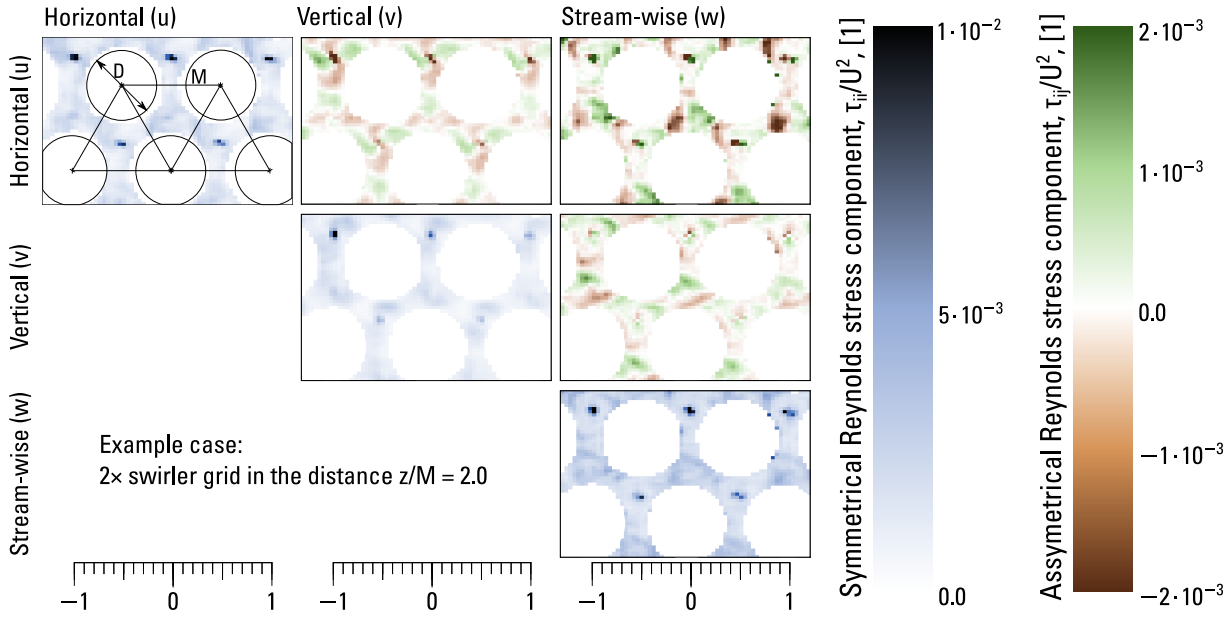

Fig. 1: Example of the spatial distribution of the individual components of the Reynolds stress tensor τ_{ij}, this tensor has 6 independent components.

, where $D = 42.2\,\mathrm{mm}$ is the diameter of fuel rods. Hence, D_h-based Reynolds number is $\mathrm{Re}_{Dh} = 6.11{\cdot}10^4$, this value can be compared with the results of Orosz et al. (2022) or Qu and Xiong (2024). Note that the wind tunnel model is up-scaled, although in many other engineering applications the model is used to be down-scaled. Anyway, we did not reach the Reynolds number of nuclear reactor, which is in order from $2.5 \cdot 10^5$ (VVER440) to $4.5 \cdot 10^5$ (VVER1000) due to the very low viscosity of water ($1.3 \cdot 10^{-7}\,\mathrm{m^2/s}$) under working conditions (pressure $12.3\,\mathrm{MPa}$ or $15.7\,\mathrm{MPa}$ respectively and temperature $268\,^\circ\mathrm{C}$ or $290\,^\circ\mathrm{C}$ respectively). Details about the swirler grid are described by Dolejš et al. (2026).

3. Anizotropy of fluctuations

The *anizotropy* (or sometimes *anisotropy*) can be calculated according to Choi and Lumley (2001), if all three components of the fluctuating velocity field are measured. The velocity signal in each direction can be decomposed to its mean and fluctuating part, $u_i = \langle u_i \rangle_t + u_i'$. The Reynolds stress tensor is

$$\tau_{ij} = \left\langle u_i' \cdot u_j' \right\rangle \tag{2}$$

The structure of this tensor is illustrated in Fig. 1, where the diagonal components are always positive and their sum (trace of the tensor) is known as turbulent kinetic energy (times one half), while the non-diagonal terms are antisymmetric, hence only 6 independent components exist in the tensor. Still, it is quite a large amount of information, see Fig. 1. This figure displays only single measuring plane in a single case. This figure is organized as components of the matrix: top left panel is τ_{xx}, top central panel displays τ_{xy} etc. Note, that we have measured at 5 downstream planes and compared 4 configurations – the base spacer grid with no swirling elements; the case where only the last grid contains swirling elements; the case where two last grids contain swirling elements; and finally the case without fuel rods to compare the behavior of free vortex with a vortex constrained between the fuel rods. To extract the most interesting information – the level of anisotropy independently of the actual orientations of the coordinate system, Lumley and Newman (1977) suggested the invariants of the tensor τ_{ij} to define the *anizotropy coefficient* F:

$$F = 1 + 9I_2 + 27I_3 \tag{3}$$

where

$$I_2 = -b_{ij} \cdot b_{ji} \quad \text{and} \quad I_3 = \frac{1}{3} b_{ij} \cdot b_{jk} \cdot b_{ki} \tag{4}$$

where b is the non-dimensional anizotropic part of Reynolds stress tensor τ

$$b_{ij} = \frac{\tau_{ij}}{\tau_{kk}} - \frac{1}{3}\delta_{ij} \tag{5}$$

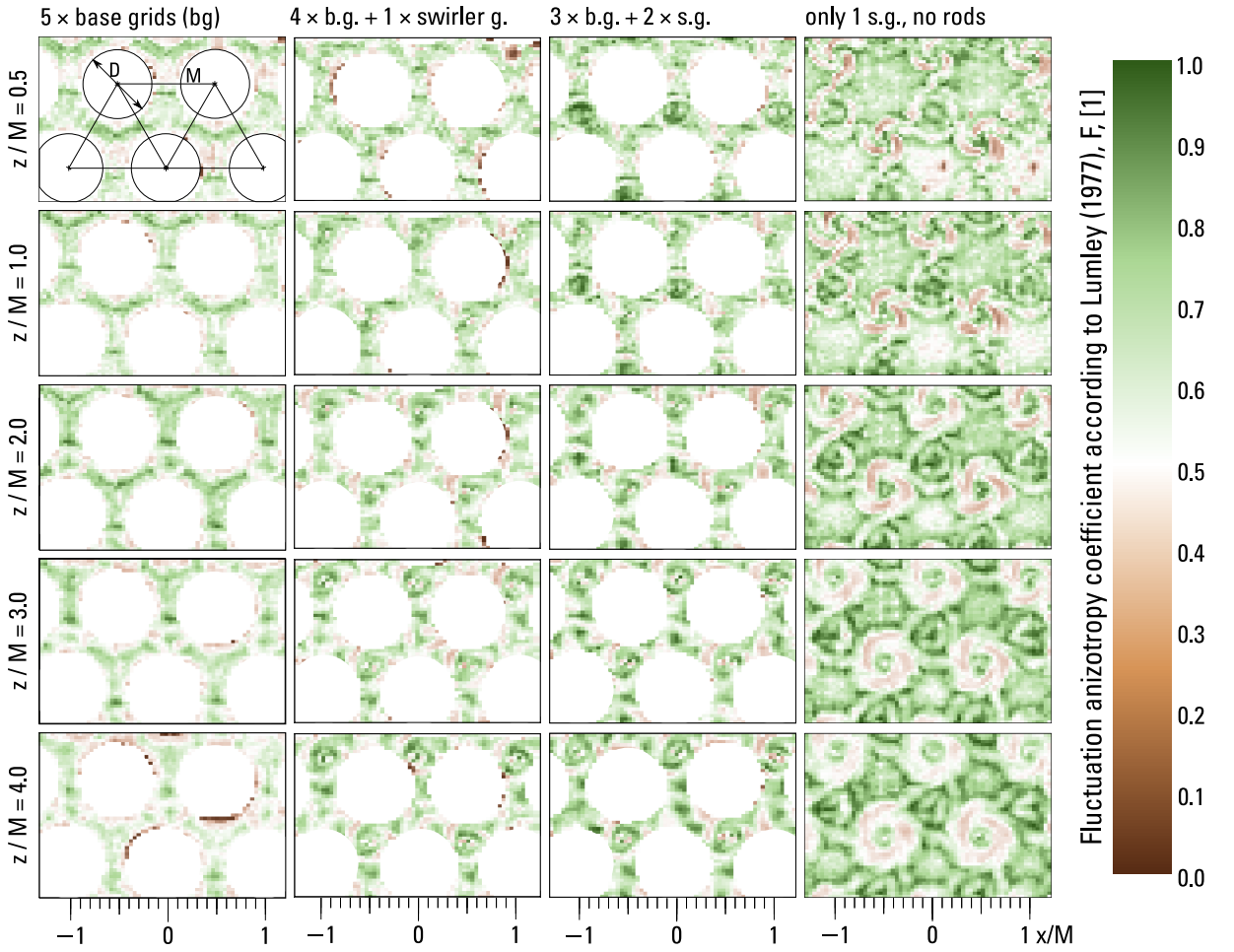

Fig. 2: Spatial map of fluctuation anisotropy coefficient as defined by Lumley and Newman (1977).

4. Results

Figure 2 displays the spatial distribution of F for the four explored cases (columns) and at five distances downstream of the grid (rows). The case past just swirler grids (the right column of Fig. 2) shows large F (green colors) almost everywhere including the areas in the for the fuel rods, where there is low turbulence level. Similarly, the area behind the circle node displays $F \in (0.6; 0.9)$ with downstream developed structure of concentric circles. The only low-anisotropy areas (brown colors in Fig. 2) lie in the envelope of vortices produced by the swirler nodes of the grid. This can be explained by the increased low-scale turbulence in the vortex envelope, which makes the fluctuations more isotropic.

In the cases with fuel rods (middle columns in Fig. 2), we see a different trend: the general level of anisotropy varies less, it is closer to 0.5 everywhere. In the areas pat swirlr nodes is the anizotropy larger; note the residuals of shear layers at the vortex envelopes also depicted by brown colors (i.e. low F).

It is clear that the presence of boundary layers at the fuel rods significantly reduces the peaks in the turbulence anisotropy. This may coincide with the fact that the large-scale coherent structures are blocked by the rods, and the smaller-scale structures, which fit into the interrod channels, display naturally lower anizotropy.

Figure 3 shows the anizotropy of two different length-scales (top row: small scales, bottom row: large scales) at single position $z = 2M$. In the case without fuel rods (right column), we see that the isotropic behavior inside the vortex envelopes is associated with large scales. With fuel rods present (first three columns), the situation is opposite: the isotropic signal of shear layers between neighboring channels comes from the small-scale fluctuations, while the large-scale ones are responsible for strongly anisotropic behavior of the shear layers and vortex centers.

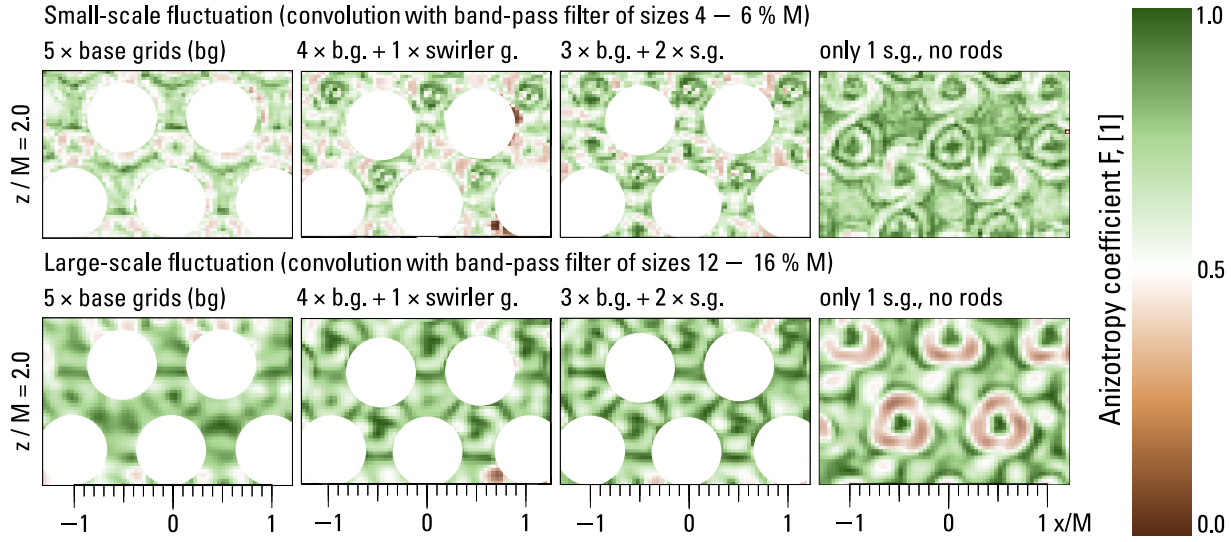

Fig. 3: Anizotropy of length-scale decomposed fields according to Duda and Uruba (2019).

5. Conclusions

The flow through a nuclear fuel assembly model is explored by using a standard method of PIV. The spacer grid contains swirling elements creating longitudinal vortices in every even inter-rod channel. We focus on the anisotropy coefficient defined by Lumley and Newman (1977). This analysis shows a significant contribution of the boundary layers formed at the fuel rods, because the turbulence in the vortex envelopes cannot evolve into full homogeneous and isotropic turbulence. The applied air-tunnel PIV methodology proves to be efficient for assessing the impact of modifications that enable rapid evaluation of geometrical changes and the optimisation of spacer-grid designs for nuclear fuel assemblies.

Acknowledgments

We would like to especially thank Elektrárna Dukovany II, a. s. for the support to present the results of our research.

References

Choi, K. and Lumley, J. (2001) The return to isotropy of homogeneous turbulence. *J. Fluid Meach.*, 436, pp. 59–84.

Dolejš, M., Duda, D., Janský, V., Mrázová, A., Uruba, V., Yanovych, V. P., Vasconcelos da Silva, I. K., and Kovalova, K. V. (2026) Vortices produced by swirl-mixing grids in nuclear fuel assembly: a wind-tunnel experiment. *Flow*, 6, pp. E8.

Duda, D. and Uruba, V. (2019) Spatial spectrum from particle image velocimetry data. *ASME J of Nuclear Rad Sci.*, 5, 030912.

Lumley, J. and Newman, G. (1977) The return to isotropy of homogeneous turbulence. *J. Fluid Meach.*, 82, pp. 161–178.

Nazififard, M. (2018) Cfd simulation of swirl flow in hexagonal rod bundle geometry by split mixing vane grid spacers. *Thermal Science*, 2018, pp. 76–76.

Nguyen, T., White, L., Vaghetto, R., and Hassan, Y. (2019) Turbulent flow and vortex characteristics in a blocked subchannel of a helically wrapped rod bundle. *Experiments in Fluids*, 60, 8.

Orosz, G. I., Magyar, B., Szerbák, D., Kacz, D., and Aszódi, A. (2022) Allegro gas cooled fast reactor rod bundle investigations with cfd and piv method. *Nuclear Engineering and Design*, 400, pp. 112062.

Qu, W. and Xiong, J. (2024) High-fidelity piv measurements of turbulent flow in reactor pressure vessel assisted by high-precision matched index of refraction technique. *Nuclear Engineering and Design*, 420, pp. 112997.

Tropea, C., Yarin, A., and Foss, J. F. (2007) *Springer Handbook of Experimental Fluid Mechanics*. Springer, Heidelberg, DE.

Turankok, N., Lohez, T., Biscay, V., and Rossi, L. (2024) Velocity and pressure fluctuations downstream analytical spacer grids: Structure and transport. *Nuclear Engineering and Design*, 430, pp. 113682.

Yanovych, V., Duda, D., Horáček, V., and Uruba, V. (2019) Research of a wind tunnel parameters by means of cross-section analysis of air flow profiles. *AIP Conference Proceedings*, 2189, 020024.